State of Charge Dependent Ordered and Disordered Phases in a Li[Ni$_{1/3}$Co$_{1/3}$Mn$_{1/3}$]O$_2$ Cathode Material

*Chi Ho Lee,‡[a]   Byeongsun Jun,‡[a]   Seung Cheol Lee [*c] and Sang Uck Lee [*a,b]*

[a] Department of Bionano Technology, Hanyang University, Ansan 15588, Republic of Korea.
[b] Department of Applied Chemistry, Center for Bionano Intelligence Education and Research, Hanyang University, Ansan 15588, Republic of Korea.
[c] Indo-Korea Science and Technology Center, Korea Institute of Science and Technology, Bangalore, 560065, India.
‡ These authors contributed equally to this work.

AUTHOR INFORMATION

Corresponding Authors: Sang Uck Lee, Seung Cheol Lee

*Email: sulee@hanyang.ac.kr (S.U.L.)
*Email: leesc@kist.re.kr (S.-C. L.)

Section A: Cluster expansion

First principles calculation is a great tool for calculating small size unit cell (roughly < 200 atoms in current computing power) at the ground state. This disadvantage that only can be used to small size unit cell can be overcome by merging the cluster expansion with Monte Carlo simulation. The cluster expansion method is useful for finding properties of a crystal when the crystal can have many different arrangements of atoms. Here, the significant assumption is that other degrees of freedom are marginal. The binary cluster expansion equation is generally expressed using polynomial model as

$$E = J_0 + J_1 \sum_i \sigma_i + J_2 \sum_{ij} \sigma_i \sigma_j + J_3 \sum_{ik} \sigma_i \sigma_k + \cdots + J_4 \sum_{ijk} \sigma_i \sigma_j \sigma_k + \cdots$$

where J, the key value of cluster expansion, represents effective cluster interactions (ECI), $\boldsymbol{\sigma}$ is the occupation variable which takes +1 or -1 for binary atoms (*e.g.* $LiNi_xCo_{1-x}O_2$ system: if the site is Ni, $\sigma=1$ and $\sigma=-1$ for Co), and the indices $\boldsymbol{i, j, k, \cdots}$ correspond to the different sites in the crystal. The number of indices indicates the number of sites existing in its clusters. We can expand previous binary cluster expansion to a multicomponent system as

$$E = J_0 + \sum_\alpha J_\alpha \Phi_\alpha^n + \sum_\beta J_\beta \Phi_\beta^n + \cdots + \sum_\gamma J_\gamma \Phi_\gamma^n + \cdots$$

where $\boldsymbol{\Phi}$ replaces σ to express atomic information using point vector and $\boldsymbol{n}$ represents the indices of the point vector which are to be multiplied. For instance, ternary system of $\boldsymbol{\Phi}$ is expressed by $[1, \tau, \tau^2]$ where value of τ is -1, 0 or 1 (*e.g.* if the $LiNi_xCo_yMn_{1-x-y}O_2$ system, Ni=-

1, Co=0, Mn=1). From the polynomial, we can estimate the unknown ECIs from several first principle calculation energies (E) and site information (σ or Φ) of clusters in the crystal. There are several methods of obtaining appropriate ECIs: structure inversion method (SIM), genetic algorithm (GA), LASSO and so on. The SIM is the classical method which includes all clusters without selection. GA is the most general way to obtain ECIs that select the effective clusters among possible clusters by minimizing cross-validation score. After we obtain ECI, we can predict energy of a structure which has not been calculated. Therefore, we can perform atomic exchange Monte Carlo simulation rapidly without first principles calculation using the popular Metropolis algorithm.

The structure in which Li content is 33% was made such that 3 Li are not adjacent to each other by removing 6 Li from the structure having 9 Li. Similarly, the Li 66% structure was prepared by interchanging the Li site and the vacant site from the Li 33% structure. This reduced structure cannot accurately represent the physical properties of the three-layer NMC structure, but it can serve as an estimate for the stable arrangement of TM due to the change of the charge state of TM resulting from the presence or absence of Li. Then, a 3×3×1 supercell was used so that a sufficient amount of transition metal could be placed in one layer. We did not maintain the composition of Ni, Mn and Co at 3:3:3. When the composition is maintained as such, the number of each TM is too small, and thus the configuration that clustered TM cannot be fully

reflected. We used genetic algorithm (GA) optimization to find the best clusters with the lowest cross-validation score in various cluster pools. The number of populations was 19, 11, 5 and 6 for Li 0%, Li 33%, Li 66% and Li 100% structures, respectively and the maximum generation was set to 200 with 0.001 tolerance. Table S1 lists the cluster expansion information and results. Selected clusters indicate the effective cluster selected after the GA is chosen from among the more than 30 clusters which containing next-adjacent TMs from the central site. The cluster information represents the atoms that make up the selected clusters. The average error (AVG Err) between predicted energy and calculated energy of test set is also provided.

Table S1. Selected clusters and average error toward the test sets (10% of total configurations) after cluster expansion using genetic algorithm.

Li (%)	The number of configurations	Selected cluster	Cluster information	AVG Err (meV/atom)
0.0	738	4-site: 2	TM2O2 0.00000 0.00000 0.00000 -0.24156 0.42510 0.22435 0.33333 0.00000 0.00000 -0.33333 0.33333 0.00000 TM3O1 0.00000 0.00000 0.00000 0.00000 0.33333 0.00000 0.09177 0.09177 0.22435 0.09177 -0.24156 0.22435	1.3
0.33	1950	2-site: 1, 3-site: 2	TM2 0.00000 0.00000 0.00000 0.33333 -0.33333 -0.00000 TM1O2 0.00000 0.00000 0.00000 -0.24156 0.09177 0.22435 0.09177 0.09177 0.22435 TM1O1Li1 0.00000 0.00000 0.00000 0.33333 -0.33333 -0.00000 0.16667 -0.16667 0.50000	3.16
0.67	1950	3-site: 1, 4-site: 1	TM2Li1 0.00000 0.00000 0.00000 0.33333 -0.33333 -0.00000 0.16667 -0.16667 0.50000	3.7

			TM1O3	
			0.00000 0.00000 0.00000	
			-0.24156 0.42510 0.22435	
			0.09177 0.09177 0.22435	
			-0.24156 0.09177 0.22435	
1.0	738	2-site: 1, 4-site: 1	TM2	4.62
			0.00000 0.00000 0.00000	
			0.33333 0.33333 0.00000	
			TM1O3	
			0.00000 0.00000 0.00000	
			0.42510 -0.24156 0.22435	
			0.09177 0.09177 0.22435	
			0.09177 -0.24156 0.22435	

Section B: Li$_{27}$[Ni$_{12}$Co$_{12}$Mn$_{12}$]O$_{72}$ structure modeling
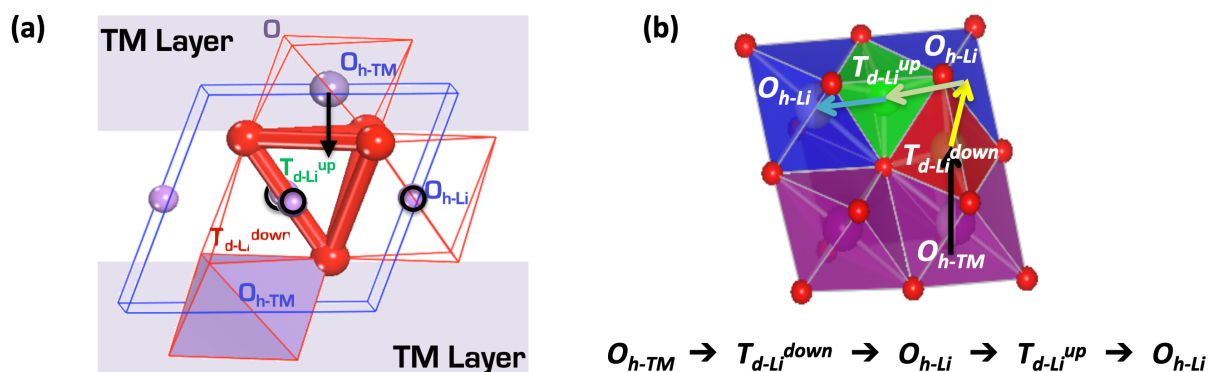
Figure S1. (a) Model structure of transition metal oxide consisting of O$_h$ and T$_d$ vacancy and occupation of TM and Li ions. (b) Schematic TM migration path from TM layer to Li layer through alternating O$_h$ and T$_d$ sites, where purple and blue are O$_h$ site at TM and Li layer, and green and red means up/down types of T$_d$ sites at Li layer.
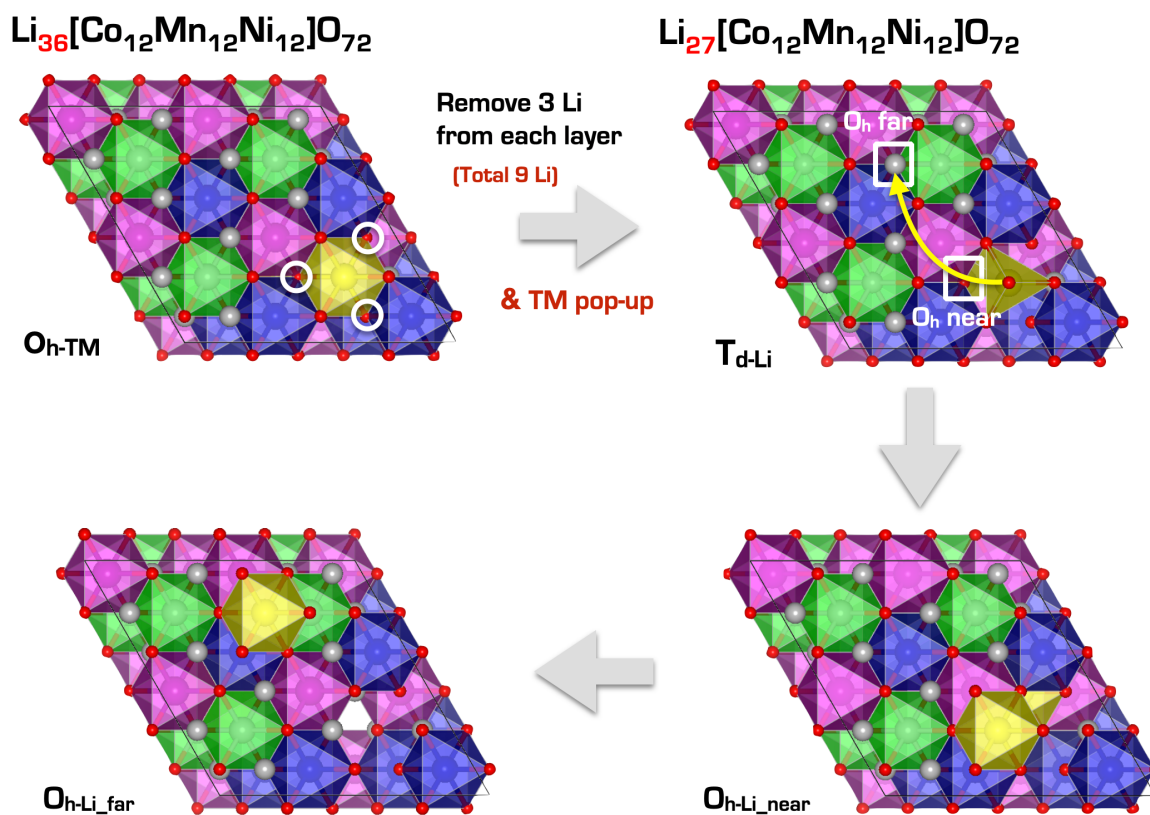
Figure S2. Progress of Li$_{27}$[Ni$_{12}$Co$_{12}$Mn$_{12}$]O$_{72}$ structure modeling and pop-up-initiated TM migration pathway. (Green, blue, purple and gray are Ni, Co, Mn and Li ions, respectively)

In transition metal (TM) oxide, oxygen anions take cubic closed packing and create two types of vacancy, O_h and T_d. TM and Li cations alternatively occupy only O_h sites rather than T_d sites forming a layered structure due to thermodynamic stability. However, although the T_d site is unstable, it can be filled by cations when the four O_h sites that face sharing with the T_d site are empty. Therefore, as shown in Figure S1(a), when three O_{h-Li} of Li layer are empty, TM of TM layer can pop-up to Li layer. Additionally, considering TM pop-up from TM layer to Li layer and ion migration, ions must pass alternatively through O_h and T_d sites (O_{h-TM} ➜ T_{d-Li}^{down} ➜ O_{h-Li} ➜ T_{d-Li}^{up} ➜ O_{h-Li}), as shown in Figure S1(b). So, in order to investigate the phase transition mechanism and relative stability during TM migration, we designed $Li_{27}[Ni_{12}Co_{12}Mn_{12}]O_{72}$ structure by removing Li around the T_d site such that TM will pop-up from each Li layer of the $Li_{36}[Ni_{12}Co_{12}Mn_{12}]O_{72}$ base structure, as shown in Figure S2.

Section C: Structural changes depending on the doping concentration

To provide additional insight in understanding doped NCM system experimentally and theoretically, we systematically calculated formation energies of Zr-doped NCM111 structures depending on the doping ratio (1.30, 2.94, 5.65, and 10.88 mol%), and intensively investigated structural changes of them attributed to the atomic size difference. The results in Figure S3 clearly reveal that there is little difference in the formation energy, lattice parameter, and local bond distance according to the doping ratio, even though the atom size of Zr is different with Co.
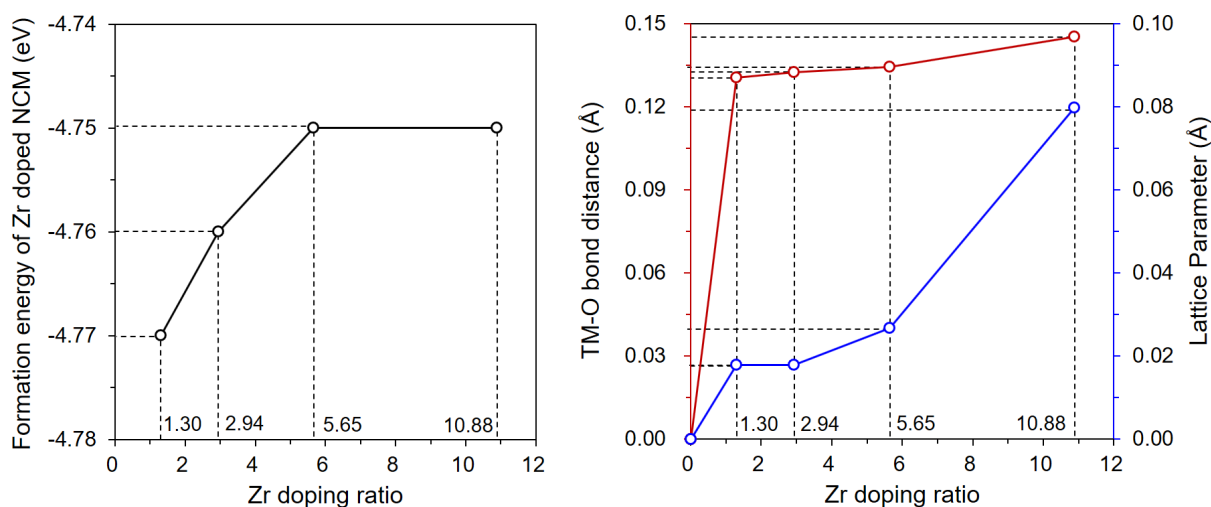
Figure S3. Difference on formation energy of Zr-doped NCM111, lattice parameter, and TM-O bond distance (TM=Co or Zr) depending on Zr doping ratio (1.30, 2.94, 5.65, and 10.88 mol%).